

Robust Decision-Making in Spatial Learning: A Comparative Study of Successor Features and Predecessor Features Algorithms

Hyunsu Lee

Abstract—Predictive map theory, one of the theories explaining spatial learning in animals, is based on successor representation (SR) learning algorithms. In the real world, agents such as animals and robots are subjected to noisy observations, which can lead to suboptimal actions or even failure during learning. In this study, we compared the performance of Successor Features (SFs) and Predecessor Features (PFs) algorithms in a noisy one-dimensional maze environment. Our results demonstrated that PFs consistently outperformed SFs in terms of cumulative reward and average step length, with higher resilience to noise. This superiority could be due to PFs' ability to transmit temporal difference errors to more preceding states. We also discuss the biological mechanisms involved in PFs learning for spatial navigation. This study contributes to the theoretical research on computational neuroscience using reinforcement learning algorithms, and highlights the practical potential of PFs in robotics, game AI, and autonomous vehicle navigation.

Index Terms—Reinforcement learning, Successor features learning, Predecessor features learning, Navigation, Noisy environment.

I. INTRODUCTION

BOTH animals and humans require navigation and decision-making skills to locate resources, avoid dangers, and ultimately thrive in their environment. An agent must utilize sensory inputs from the environment, such as visual or auditory cues, and update its internal representation of the environment based on these inputs in order to navigate effectively. Because these inputs are associated with rewards or punishments provided by the environment, the animal must remember their associations and build an internal model.

Mammals, birds, and reptiles use the hippocampus to encode spatial representations in order to organize and learn about relationships [1]–[4]. In 1971, O'Keefe and Dostrovsky demonstrated that place cells in the rodent hippocampus show firing patterns specific to certain locations, revealing a spike code for spatial information [5]. This finding led to the theory that the hippocampus serves as a cognitive map for spatial navigation [6]. More recently, the discovery of grid cells in the entorhinal cortex added another layer of complexity to our understanding of spatial navigation [7], [8]. Grid cells

are neurons that fire in a repeating triangular or hexagonal pattern, creating a grid-like representation of space. Together with place cells, grid cells play a crucial role in the brain's ability to navigate and remember spatial environments.

The discovery of place cells and grid cells in the hippocampus has led to the development of various hypotheses to explain how the brain processes spatial information [9]. One such theory is the predictive map theory proposed by Stachenfeld [10], which is based on the successor representation (SR) learning algorithm. The concept of SR learning includes the dissection of rewards and state transitions [11]. Consequently, SR learning involves representing the future expected occupancy of each state, under a particular policy. This representation enables the agent to efficiently compute the expected value of all states given a policy without carrying out an exhaustive search of the state space. The predictive map theory has been proposed as a powerful explanatory and predictive model for understanding the neural mechanisms involved in spatial learning and navigation. However, despite its success in providing a theoretical framework, there is a lack of research on how robust SR learning is in real-world settings where noise is inevitable, which is important in terms of neurobiological applications where animals are solving navigation problems in the real world.

Reinforcement learning (RL) is a computational approach that describes the interaction between agents and their environment, with the aim of optimizing reward signals. In this framework, agents learn to associate their actions with outcomes that lead to positive or negative rewards and use this knowledge to guide their future behavior. The ultimate goal of RL is to discover the optimal policy, or the mapping between states and actions, that maximizes the expected cumulative reward over time. The weights in RL are determined by the temporal difference (TD) error between the predicted and actual state values, which represents the reward prediction error and is believed to reflect the pattern of dopamine release [12]–[14]. A variant of the TD learning algorithm is TD(λ), which introduces the concept of eligibility traces, which show similarities to the neurobiological mechanism of synaptic tagging [15]. Although predecessor representation (PR) learning [16], [17], an algorithm that combines TD(λ) learning and SR learning, has already been proposed, its potential neurobiological implications and robustness in noisy environments have received relatively little attention.

H. Lee is with the Faculty of Department of Medical Informatics, School of Medicine, Keimyung University, Daegu, Republic of Korea.

This work has been submitted to the IEEE for possible publication. Copyright may be transferred without notice, after which this version may no longer be accessible.

In this paper, we compare the performance of the successor features (SFs) and predecessor features (PFs) algorithms, which are linear approximation extensions of SR and PR learning, in noisy environments. In Section II, we provide a detailed explanation of the *Markov decision processes* and delve into the mathematical and computational aspects of the SR learning and SFs algorithms. In Section III, we present the implementation of the PFs learning algorithm. In Section IV, we define a noisy one-dimensional maze environment, analyze and contrast the performance of the SFs and PFs algorithms in the noisy environment. In Section V, we introduce prior research related to SFs and PFs algorithms and reinforcement learning in noisy environments. Finally, in Section VI, we discuss the theoretical explanation for the strength of the PFs algorithm, mention the limitations of this study, and discuss the implications of our findings for AI and neuroscience research.

II. BACKGROUND AND PROBLEM FORMULATION

A. Markov decision processes

In this paper, we assume that RL agents interact with the environment through *Markov decision processes* (MDPs). The MDP used in this paper is a tuple $M := (\mathcal{S}, \mathcal{A}, R, \gamma)$ consisting of the following elements. The set \mathcal{S} is the states (i.e., information about the space), and the set \mathcal{A} is the space of actions that the agent can take. A function $R(s)$ maps the immediate reward received in state s . The discount factor $\gamma \in [0, 1)$ is a weight that reduces the value of future rewards.

The main task of the RL agent is to find a policy function that maximizes the total discounted reward, also known as the return $G_t = \sum_{i=t}^{\infty} \gamma^{i-t} R_{i+1}$, where $R_t = R(S_t)$. To solve this problem, we typically use *dynamic programming* methods to define and compute a value function $V^\pi(s) := \mathbb{E}^\pi[G_t | S_t = s]$ that depends on the policy π . The value function can be estimated by an approximation function $v^\mathbf{w}(s) \approx v^\pi(s)$ parameterized by a weight vector $\mathbf{w} \in \mathbb{R}^d$. To update the weight vector, TD learning can be utilized as follows: $\mathbf{w}_{t+1} = \mathbf{w}_t + \alpha[R_{t+1} + \gamma v_\mathbf{w}(s_{t+1}) - v_\mathbf{w}(s_t)] \nabla_{\mathbf{w}} v_\mathbf{w}(s_t)$.

TD(0) refers to an algorithm that uses the typical one-step TD update rule as mentioned above, while TD(λ) refers to an classic algorithm that uses a eligibility trace based on past experience. The update rule for TD(λ) is defined as $\mathbf{w}_{t+1} = \mathbf{w}_t + \alpha \delta_t \mathbf{e}_t$, where $\delta_t = R_{t+1} + \gamma v_\mathbf{w}(s_{t+1}) - v_\mathbf{w}(s_t)$ is referred to TD error and $\mathbf{e}_t = \gamma \lambda \mathbf{e}_{t-1} + \nabla_{\mathbf{w}} v_\mathbf{w}(s_t)$ is referred to the eligibility trace, where λ indicates the trace decay parameter.

B. Successor features learning

The core idea of SR learning is that the value function can be decomposed into the expected visiting occupancy and reward of the successor state s' as follows: $V^\pi(s) = \sum_{s'} \mathbb{E}^\pi[\sum_{i=t}^{\infty} \gamma^{i-t} \mathbb{I}(S_i = s') R(s') | S_t = s] = \sum_{s'} \mathbf{M}(s, s') R(s')$, where $\mathbb{I}(S_i = s')$ returns 1 if the agent visits the successor state s' at time t , and 0 otherwise. Thus, $\mathbf{M}(s, \cdot)$ represents the discounted expectation of a visit from state s to its successor states, which can be called a successor state vector, or more generally, SFs.

Similar to how we used a weight vector \mathbf{w} to estimate the value function, we can use a weight matrix and vector

to estimate the $\mathbf{M}(s, \cdot)$ and $R(s')$, respectively. In the tabular environment $\mathbb{R}^{|\mathcal{S}|}$, we can represent the state vector as a simple one-hot vector $\phi(s)$. Thus, we can factorize the reward vector as $R(s) = \phi(s) \cdot \mathbf{w}^r$ and the SFs as $\mathbf{M}(s, \cdot) = \mathbf{W}^{sf} \phi(s) := \psi^\mathbf{W}(s)$. Therefore, we can rewrite the value function under the policy π as follow: $V^\pi(s) = \psi^\pi(s) \cdot \mathbf{w}^r$, and the value approximation function as follow: $V^\mathbf{W}(s) = \psi^\mathbf{W}(s) \cdot \mathbf{w}^r$.

Using TD update rules, we can update \mathbf{w}^r and \mathbf{W}^{sf} as follows:

$$\mathbf{w}_{t+1}^r = \mathbf{w}_t^r + \alpha_r (R_t - \phi(s) \cdot \mathbf{w}_t^r) \phi(s) \quad (1)$$

$$\mathbf{W}_{t+1}^{sf} = \mathbf{W}_t^{sf} + \alpha_W [\phi(s_t) + \gamma \psi^\mathbf{W}(s_{t+1}) - \psi^\mathbf{W}(s_t)] \otimes \phi(s_t) \quad (2)$$

III. PREDECESSOR FEATURES LEARNING

Similarly to how the TD(0) algorithm can be converted into TD(λ) by using the eligibility trace, the incorporation of SFs with the eligibility trace can result in the production of PFs. The eligibility trace can be updated by the one-hot state vector $\phi(s)$ as follow: $\mathbf{e}_t = \gamma \lambda \mathbf{e}_{t-1} + \phi(s_t)$. Therefore, weight matrix of PFs update rule can be written as follows:

$$\mathbf{W}_{t+1}^{pf} = \mathbf{W}_t^{pf} + \alpha_W [\phi(s_t) + \gamma \psi^\mathbf{W}(s_{t+1}) - \psi^\mathbf{W}(s_t)] \otimes \mathbf{e}_t \quad (3)$$

where we used a linear approximation as $\psi^\mathbf{W}(s) = \mathbf{W}^{pf} \phi(s)$ for simplicity. It is worth noting that by using a one-hot state feature vector, we can consider PFs and PR learning to be highly analogous. Therefore, we can present an example algorithms of predecessor feature as below.

Algorithm 1 Predecessor feature learning

```

procedure PF(episodes,  $\mathbf{W}^{pf}$ ,  $\mathbf{w}^r$ ,  $\lambda$ ,  $\alpha_W$ ,  $\alpha_r$ )
  initialize  $\mathbf{W}^{pf}$ ,  $\mathbf{w}^r$ 
  for episode in 1..n do
     $s_t \leftarrow$  initial state of episode
     $\mathbf{e} \leftarrow 0$  (eligibility trace reset)
    for pair  $(s_t, s_{t+1})$  and reward  $r$  in episode do
       $\mathbf{e} \leftarrow \mathbf{e} + \phi(s_t)$ 
       $\delta^{pf} \leftarrow \phi(s_t) + \gamma \psi^\mathbf{W}(s_{t+1}) - \psi^\mathbf{W}(s_t)$ 
       $\delta^r \leftarrow r - \phi(s_{t+1}) \cdot \mathbf{w}^r$ 
       $\mathbf{W}^{pf} \leftarrow \mathbf{W}^{pf} + \alpha_W \delta^{pf} \otimes \mathbf{e}$ 
       $\mathbf{w}^r \leftarrow \mathbf{w}^r + \alpha_r \delta^r \phi(s_{t+1})$ 
     $\mathbf{e} \leftarrow \gamma \lambda \mathbf{e}$ 
  return  $\mathbf{W}^{pf}$ ,  $\mathbf{w}^r$ 

```

IV. EXPERIMENTAL DESIGN AND RESULTS

A. Environment with noise

In this study, we designed a one-dimensional maze environment with noise in the observation vector to compare the performance of SR and PR learning algorithms. The maze consists of twenty states, where the agent starts from state 1 and must reach state 20 to receive a reward of 1. The agent's action space consists of two possible actions: move right or move left. The agent was provided with a one-hot state feature

vector to represent its current state. However, to account for the effects of sensor noise commonly encountered in real-world scenarios, we added a Gaussian noise term to the observation vector \mathbf{o}_t received by the agent in each state as following:

$$\mathbf{o}_t = \phi(s_t) + \epsilon_t, \quad \epsilon_t \sim \mathcal{N}(\mathbf{0}, \sigma^2 \mathbf{I}) \quad (4)$$

where ϵ_t is the Gaussian noise vector with zero mean and covariance matrix $\sigma^2 \mathbf{I}$, where \mathbf{I} is the identity matrix. Since the σ regulates the level of noise in the \mathbf{o}_t , as σ rises, the \mathbf{o}_t grows noisier.

To evaluate the performance of the agents in this noisy environment, we conducted a total of 20 runs of 200 episodes each. Two metrics were used to measure the effectiveness and robustness of the agents: the average cumulative reward obtained over 200 episodes and the average number of steps taken to reach the goal state within 100 steps. In each episode, the agent starts from state 1 and continues to take actions until it reaches state 20 or until a maximum of 100 steps is reached. The metrics provide a quantitative measure of the agents' ability to navigate the noisy environment and reach the goal state.

The noise level of the observation vector was adjusted with σ and tested the SFs and PFs algorithms with different noise levels to confirm the robustness of the results. By adjusting the σ from 0 to 0.15 in 0.03 intervals, we explored environments that were challenging enough to differentiate the performance of the algorithms.

B. Comparison of PFs and SFs Algorithms in Noisy and Noiseless Environments

In this section, we present the results of our study comparing the performance of SFs and PFs learning algorithms in a noisy one-dimensional maze environment. Our results showed that PFs learning outperformed SFs even in the absence of noise, as evidenced by more cumulative reward (Figure 1) and a faster decrease in average step length (Figure 2). The average cumulative reward was 191.75 (5.78) for PFs and 170.85 (16.33) for SFs, and the average step length across episodes was 27.38 (2.10) for PFs and 35.52 (6.42) for SFs. In both metrics, PFs significantly outperformed SFs according to the results of the two-sample t-test (Table I and II).

When we increased the noise level of the observation vector by $\sigma = 0.03$, the cumulative reward of SFs learning decreased significantly, while the cumulative reward of PFs learning decreased less (Figure 3). The average cumulative reward was 183.70 (6.20) for PFs and 89.35 (22.04) for SFs. Also, the average step length decreased faster in PFs learning than in SFs learning (Figure 4). The average step length across episodes was 48.22 (1.64) for PFs and 81.13 (5.56) for SF. When the noise level reaches $\sigma = 0.15$, we can see that the noise prevents both algorithms from learning properly, causing the step length to approach the maximum value of 100 (Figure 6 and Table II). At lower noise levels, such as $\sigma = 0.06, 0.09$, and 0.12 , the PFs algorithm maintained its dominance (Figure 5 and Table I).

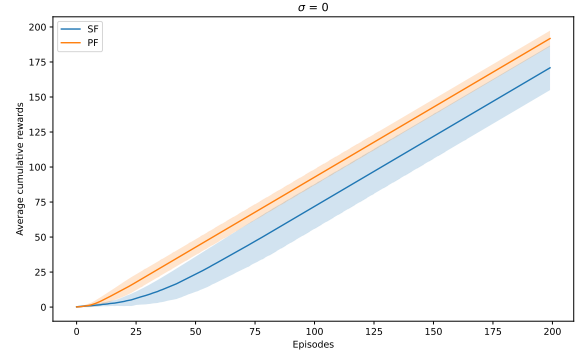


Fig. 1. Average cumulative reward in a noiseless one-dimensional maze ($\sigma = 0$). The PFs algorithm (orange line) earned more cumulative reward than the SFs algorithm (blue line). The shade of each color represents the standard deviation.

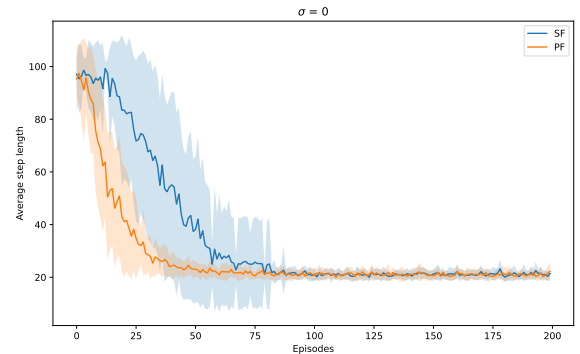


Fig. 2. Average step length in a noiseless one-dimensional maze ($\sigma = 0$). The PFs algorithm (orange line) decreases faster the step length than the SFs algorithm (blue line). The shade of each color represents the standard deviation.

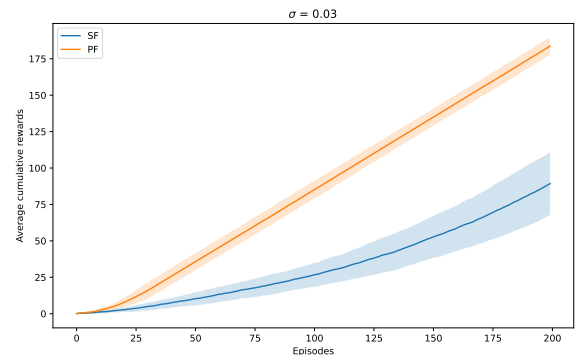


Fig. 3. Average cumulative reward in a one-dimensional maze with small noise ($\sigma = 0.03$). The PFs algorithm (orange line) earned more cumulative reward than the SFs algorithm (blue line). The shade of each color represents the standard deviation.

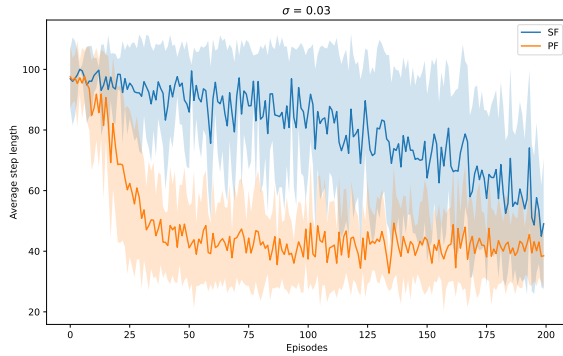


Fig. 4. Average step length in a one-dimensional maze with small noise ($\sigma = 0.03$). The PFs algorithm (orange line) decreases faster the step length than the SFs algorithm (blue line). The shade of each color represents the standard deviation.

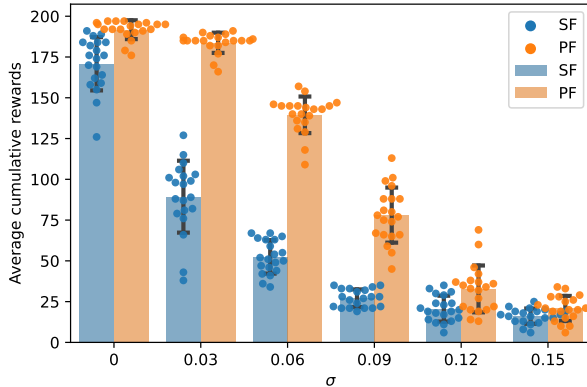


Fig. 5. Comparison of average cumulative reward between PFs and SFs algorithms over varying levels of observation vector. As the noise level increases, PFs consistently outperforms SFs in terms of cumulative reward. The x-axis represents the noise level with σ values ranging from 0 to 0.3. The y-axis represents the average cumulative reward obtained by the agents at the end of 200 episodes. The blue bars and orange bars represent the average cumulative reward for SFs and PF, respectively. The blue dots and orange dots represent individual episode scores for SFs and PF, respectively. Error bars represent the standard deviation of the mean.

TABLE I
THE AVERAGE CUMULATIVE REWARD BETWEEN PFs AND SFs
ALGORITHMS WITH CORRESPONDING P-VALUES

| σ | PF | SF | p value |
|----------|---------------|---------------|------------------------|
| 0 | 191.75(5.78) | 170.85(16.33) | 3.84×10^{-6} |
| 0.03 | 183.70(6.20) | 89.35(22.04) | 1.54×10^{-20} |
| 0.06 | 139.55(11.21) | 52.45(10.26) | 1.40×10^{-25} |
| 0.09 | 78.05(16.88) | 27.05(5.43) | 2.04×10^{-15} |
| 0.12 | 32.80(14.36) | 20.70(7.93) | 2.12×10^{-3} |
| 0.15 | 20.80(7.86) | 16.10(4.68) | 2.48×10^{-2} |

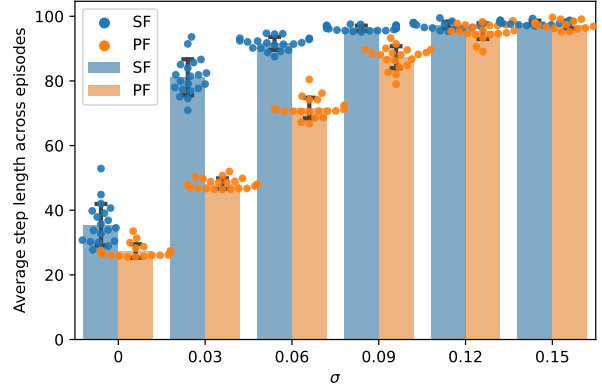


Fig. 6. Comparison of average step length across episodes between PFs and SFs algorithms over varying levels of observation vector. As the noise level increases, PFs consistently outperforms SFs in terms of average step length. The x-axis represents the noise level with σ values ranging from 0 to 0.3. The y-axis represents the average length across 200 episodes. The blue bars and orange bars represent the average cumulative reward for SFs and PF, respectively. The blue dots and orange dots represent individual episode scores for SFs and PFs, respectively. Error bars represent the standard deviation of the mean.

TABLE II
THE AVERAGE STEP LENGTH ACROSS EPISODES BETWEEN PFs AND SFs
ALGORITHMS WITH CORRESPONDING P-VALUES

| σ | PF | SF | p value |
|----------|-------------|-------------|------------------------|
| 0 | 27.38(2.10) | 35.52(6.42) | 3.85×10^{-6} |
| 0.03 | 48.22(1.64) | 81.13(5.56) | 1.94×10^{-25} |
| 0.06 | 71.60(3.20) | 91.62(1.99) | 2.08×10^{-24} |
| 0.09 | 87.32(3.40) | 96.31(0.78) | 5.56×10^{-14} |
| 0.12 | 95.40(2.41) | 97.28(1.03) | 2.84×10^{-3} |
| 0.15 | 97.42(1.22) | 98.01(0.63) | 6.09×10^{-2} |

V. RELATED WORKS

Recent studies have highlighted the advantages of the SFs approach, which decouples the feature representation from the reward function and is thus suitable for knowledge transfer between domains. In the paper that first coined the term SFs, they demonstrated that SFs facilitate the exchange of information across tasks and provide performance guarantees for the transferred policy even before learning begins [18]. Another notable advancement is the universal successor features approximators, which combine the strengths of universal value function approximators, SFs, and generalized policy improvement [19]. Furthermore, Lehnert [20] showed that SFs learning is equivalent to model-free learning, and that SFs encode model reductions that compress the state space by creating state partitions of bisimilar states. Together, these studies demonstrate the usefulness and versatility of SFs in reinforcement learning.

Pitis [17] introduced the concept of "source traces" as an application of eligibility traces to SR learning. They demonstrated the convergence of a TD(λ)-like source learning algorithm and developed a novel algorithm for learning the source (SR) map, which outperformed previous approaches. Bailey [16] also proposed an algorithm based on the same idea as proposed in this paper, naming it "predecessor features". The

predecessor features algorithm was shown to be applicable to both tabular and feature representations, and demonstrated to outperform the "ExpectedTrace" [21] algorithm in the Cartpole task. However, it has not been compared to the SFs algorithm in a noisy environment.

In a seminal investigation into the effects of noise on reinforcement learning, Pendris [22] examined the impact of noise perturbations on five distinct RL algorithms. The study's results indicate that Q-learning learns significantly slower in noisy environments. In response, Pendris proposed two new algorithms, P-trace and Q-trace, which were based on Q-learning and demonstrated faster learning on the noisy Cartpole task. Fox [23] proposes G-learning, a new off-policy learning algorithm that regularizes the noise in the space of optimal actions by penalizing deterministic policies at the beginning of the learning. Sun [24] studies the training robustness of distributional RL against noisy state observations and shows that distributional RL enjoys better training robustness compared with its expectation-based counterpart across various state observation noises.

VI. DISCUSSION AND CONCLUSION

Our results showed that PFs learning outperformed SFs learning even in the absence of noise, as evidenced by a higher cumulative reward and a faster decrease in average step length. In both metrics, PFs significantly outperformed SFs according to the results of the two-sample t-test. To the best of our knowledge, our study is the first to directly compare SFs and PFs learning algorithms in a noisy one-dimensional maze environment and assess their performance across multiple metrics and levels of noise. These results have significant implications for elucidating the neural mechanisms underlying navigation and decision-making in noisy environments, and have the potential to inform the development of more resilient artificial intelligence systems.

Previous research has suggested that SR learning and its extension, SFs learning, are a biologically plausible mechanism for decision-making and navigation, given its ability to represent the expected future occupancy of states in a spatial environment [10], [25]. However, the present study suggests that PFs learning, which represents the expected past occupancy of states, may be a more effective mechanism for decision-making and navigation. Interestingly, the idea of propagating TD errors to a larger number of predecessor states in PFs learning is reminiscent of the synaptic tagging mechanism in the brain, which involves the tagging of certain synapses with a protein to enable the storage of long-term memories [26]. This mechanism is similar to the concept of eligibility traces in RL, which assign credit to previous states based on their temporal proximity to the current state. The decoupling of feature representation from the reward function in PFs learning may allow for a more efficient and flexible tagging of synapses, similar to how the ability to propagate TD errors in the feature representation of PFs learning allows for a more accurate and robust credit assignment. Future research could explore the potential for PFs learning to shed light on the biological mechanisms of memory storage and retrieval.

In the context of learning cognitive maps, the SFs learning algorithm can be seen as a prospective approach that prioritizes predicting the next state. In contrast, the PFs learning algorithm can be considered a retrospective approach that places greater emphasis on connections to past states. A recently published study suggests that the orbitofrontal cortex acquires knowledge about both prospective and retrospective contiguity, while the hippocampus is responsible for learning sequences that are both prospective and retrospective by utilizing the concepts of SR and PR [27]. These findings suggest that both prospective and retrospective approaches are critical for successful navigation, and understanding the neural mechanisms underlying cognitive maps' learning can inform the development of more efficient and robust RL algorithms.

Nevertheless, our study revealed that PFs learning outperforms SFs learning in noisy environments. One of the key advantages of PFs learning is its ability to propagate TD errors to a larger number of prior states. Unlike SFs learning, which only assigns credit to the most recent events, PFs learning maintains an approximate representation of the expected sum of past occupancies, allowing it to propagate TD errors accurately to more previous states than traditional methods. This could explain why PFs learning remained superior to SFs learning in the presence of noise. From a neurobiological perspective, a potential mechanism for PFs learning is through the modulation of neuromodulatory systems such as dopamine and norepinephrine, which are known to play an important role in RL. For example, studies have shown that dopamine release in response to reward prediction errors follows a temporally diffuse pattern, suggesting that dopamine may be involved in propagating information about reward to multiple prior states [28], [29]. Similarly, norepinephrine has been shown to enhance the representation of past events in neural networks, which may facilitate the propagation of TD errors to more distant states [30].

Furthermore, PFs learning has been shown to have higher sample efficiency than SFs learning, requiring fewer episodes to converge to the optimal policy. This is because PFs learning utilizes the entire trajectory of experiences, while SFs learning only considers the most recent experiences. This may explain why PFs learning outperformed SFs learning in experimental settings with a limited number of episodes used to evaluate the algorithms. Overall, our findings suggest that the advantages of PFs learning over SFs learning in noisy environments could lead to more efficient and robust real-world applications of RL algorithms.

However, this study also has limitations that should be acknowledged. The use of a simplified one-dimensional maze environment may not fully capture the complexities of real-world applications, and the lack of comparison to other RL algorithms leaves open the possibility that there may be other algorithms that perform even better in noisy environments. These limitations suggest potential directions for future research, such as exploring the performance of these algorithms in more diverse and challenging environments. Future research on comparing SFs and PFs learning could explore the effectiveness of these mechanisms in more complex environments, such as mazes with multiple goals and obstacles. Additionally,

further investigation is needed to understand the underlying neural mechanisms of SFs and PFs learning and how they relate to biological systems, particularly the hippocampus.

In conclusion, our study highlights the neurobiological implications of PFs learning for navigating and making robust decisions in noisy environments. By propagating TD errors to a larger number of prior states, PFs learning may better reflect the underlying mechanisms of synaptic tagging and neuromodulation involved in real-world navigation. Incorporating PFs learning into the design of autonomous agents could lead to the development of more biologically-inspired and effective algorithms for navigating noisy and unpredictable environments.

ACKNOWLEDGMENTS

This study was supported by the National Research Foundation of Korea(NRF) grant funded by the Korea government(MSIT; Ministry of Science and ICT)(No. NRF-2017R1C1B507279). The author would like to thank ChatGPT for their assistance in editing and improving the language of the paper, as well as for their helpful brainstorming sessions.

REFERENCES

- [1] F. Rodríguez, J. C. López, J. P. Vargas, Y. Gómez, C. Broglio, and C. Salas, "Conservation of spatial memory function in the pallial forebrain of reptiles and ray-finned fishes," *The Journal of Neuroscience*, vol. 22, pp. 2894–2903, 2002.
- [2] F. Rodríguez, J. López, J. Vargas, C. Broglio, Y. Gómez, and C. Salas, "Spatial memory and hippocampal pallium through vertebrate evolution: insights from reptiles and teleost fish," *Brain Research Bulletin*, vol. 57, pp. 499–503, 2002.
- [3] H. Fotowat, C. Lee, J. J. Jun, and L. Maler, "Neural activity in a hippocampus-like region of the teleost pallium is associated with active sensing and navigation," *eLife*, vol. 8, 2019.
- [4] G. F. Striedter, "Evolution of the hippocampus in reptiles and birds," *J. Comp. Neurol.*, vol. 524, pp. 496–517, 2015.
- [5] J. O'Keefe and J. Dostrovsky, "The hippocampus as a spatial map. preliminary evidence from unit activity in the freely-moving rat." *Brain Res.*, vol. 34, pp. 171–175, 1971.
- [6] J. O'Keefe and L. Nadel, *The Hippocampus as a Cognitive Map*. Oxford University Press, USA, 1978.
- [7] T. Hafting, M. Fyhn, S. Molden, M.-B. Moser, and E. I. Moser, "Microstructure of a spatial map in the entorhinal cortex." *Nature*, vol. 436, pp. 801–806, 2005.
- [8] M. Fyhn, S. Molden, M. P. Witter, E. I. Moser, and M.-B. Moser, "Spatial representation in the entorhinal cortex." *Science*, vol. 305, pp. 1258–1264, 2004.
- [9] J. Whittington, D. McCaffary, J. Bakermans, and T. Behrens, "How to build a cognitive map." *Nat. Neurosci.*, 2022.
- [10] K. L. Stachenfeld, M. M. Botvinick, and S. J. Gershman, "The hippocampus as a predictive map." *Nature Neuroscience*, vol. 7, p. 1951, Oct 2017.
- [11] P. Dayan, "Improving generalization for temporal difference learning: The successor representation," *Neural Computation*, vol. 5, no. 4, p. 613–624, 1993.
- [12] W. Dabney, Z. Kurth-Nelson, N. Uchida, C. Starkweather, D. Hassabis, R. Munos, and M. Botvinick, "A distributional code for value in dopamine-based reinforcement learning." *Nature*, vol. 577, pp. 671–675, 2020.
- [13] W. Schultz, "Predictive reward signal of dopamine neurons," *J. Neurophysiol.*, vol. 80, pp. 1–27, 1998.
- [14] M. P. H. Gardner, G. Schoenbaum, and S. J. Gershman, "Rethinking dopamine as generalized prediction error," *Proceedings of the Royal Society B: Biological Sciences*, vol. 285, p. 20181645, 2018.
- [15] S. Gershman, "The successor representation: Its computational logic and neural substrates." *J. Neurosci.*, vol. 38, pp. 7193–7200, 2018.
- [16] D. Bailey and M. Mattar, "Predecessor features," *arXiv preprint arXiv:2206.00303*, 2022.
- [17] S. Pitis, "Source traces for temporal difference learning," *Proceedings of the AAAI Conference on Artificial Intelligence*, vol. 32, 2018.
- [18] A. Barreto, W. Dabney, R. Munos, J. J. Hunt, T. Schaul, H. Van Hasselt, and D. Silver, "Successor features for transfer in reinforcement learning," *31st Conference on Neural Information Processing Systems*, 2017.
- [19] D. Borsa, A. Barreto, J. Quan, D. Mankowitz, R. Munos, H. V. Hasselt, D. Silver, and T. Schaul, "Universal successor features approximators," *International Conference on Learning Representations*, 2018.
- [20] L. Lehnert and M. L. Littman, "Successor features combine elements of model-free and model-based reinforcement learning," *The Journal of Machine Learning Research*, vol. 21, no. 1, p. 8030–8082, 2020.
- [21] H. v. Hasselt, S. Madjiheum, M. Hessel, D. Silver, A. Barreto, and D. Borsa, "Expected eligibility traces," *arXiv*, p. 2007.01839v2, 2020.
- [22] M. D. Pendrith and C. Sammut, *On reinforcement learning of control actions in noisy and non-Markovian domains*, Technical Report, UNSW-CSE-TR-9410. Sydney, Australia: The University of New South Wales, 1994.
- [23] R. Fox, A. Pakman, and N. Tishby, "Taming the noise in reinforcement learning via soft updates," *arXiv32nd Conference on Uncertainty in Artificial Intelligence (UAI 2016)*, p. 1512.08562v4, 2015.
- [24] K. Sun, Y. Liu, Y. Zhao, H. Yao, S. Jui, and L. Kong, "Exploring the training robustness of distributional reinforcement learning against noisy state observations," *arXiv*, p. 2109.08776v4, 2021.
- [25] H. Lee, "Toward the biological model of the hippocampus as the successor representation agent." *Biosystems*, p. 104612, 2022.
- [26] W. Gerstner, M. Lehmann, V. Liakoni, D. Corneil, and J. Brea, "Eligibility traces and plasticity on behavioral time scales: Experimental support of neohebbian three-factor learning rules." *Front Neural Circuits*, vol. 12, p. 53, 2018.
- [27] V. K. Nambodiri and G. Stuber, "The learning of prospective and retrospective cognitive maps within neural circuits." *Neuron*, vol. 109, pp. 3552–3575, 2021.
- [28] T. Shindou, M. Shindou, S. Watanabe, and J. Wickens, "A silent eligibility trace enables dopamine-dependent synaptic plasticity for reinforcement learning in the mouse striatum," *Eur. J. Neurosci.*, vol. 49, pp. 726–736, 2019.
- [29] W. Pan, R. Schmidt, J. Wickens, and B. Hyland, "Dopamine cells respond to predicted events during classical conditioning: evidence for eligibility traces in the reward-learning network." *J. Neurosci.*, vol. 25, pp. 6235–6242, 2005.
- [30] S. Hong, L. Mesik, C. Grossman, J. Cohen, B. Lee, D. Severin, H. Lee, J. Hell, and A. Kirkwood, "Norepinephrine potentiates and serotonin depresses visual cortical responses by transforming eligibility traces." *Nat Commun*, vol. 13, p. 3202, 2022.



Hyunsu Lee, a dynamic and innovative Assistant Professor, is currently utilizing his expertise in Medical Informatics at Keimyung University, School of Medicine to further his cutting-edge research in the field of artificial intelligence. Driven by a passion for exploring the intersection of neuroscience and machine learning, his current research endeavors are focused on the medical and neuroscientific applications of reinforcement learning algorithms.